A R C H I V E O F M E C H A N I C A L E N G I N E E R I N G

Volume 68 2021 Number 2

DOI: 10.24425/ame.2021.137047

Key words: excavation shelter, fire, numerical analysis, part-time processes

Adam Baryłka [1]

Effort of the protective structure of the shelter under the influence of an external fire

The paper presents a numerical analysis carried out to determine the influence of the ground surface fire on the strain level of shelter housing with the ground cover. It is assumed that the underground shelter is longitudinal and the fire spans on an extensive area. The area surrounding the housing was treated as a material with average constant thermodynamic values. The heating and cooling processes were described on the basis of the Fourier's equation concerning heat conduction in consideration on material, ground and concrete heterogeneous nature. The numeric analysis was carried out in two stages. In the first stage, a quasi-stationary initial temperature distribution was sought in the ground centre and shelter shield. In the second stage of analysis, the fire effect was considered according to the time profile of temperature variation in object.

1. Introduction

In many building structures, hazards are encountered due to sudden ignition or explosion of gas, explosion of hot liquid or vapor, contact with hot objects, contact with electric arc, etc. Thermal hazards in these emergencies can have high intensities exceeding 100 kW/m^2 and 1000°C. In this paper, fires in structures of special interest such as shelters are modelled. There are few publications on shelters because they are usually strategic facilities for companies, or the military. The presented analysis is one of the few works on this type of issues. Own numerical software was used, prepared for simulation of temperature distribution from the fire environment to the shelter interior. Mathematical model describes unsteady, two-dimensional heat conduction through different types of media.

Fire incidents in buildings are one of the most dangerous hazards when it comes to evacuation safety. In order to reduce the aftermath of fire in buildings, systems

✉ Adam Baryłka, e-mail: biuro@crb.com.pl

[1] Centre of Construction Expertise, Warsaw, Poland. ORCID: 0000-0002-0181-6226

are designed to improve the fire evacuation safety [1, 2]. Evacuation safety is related to a number of sub-issues. One of them is a properly selected escape route, during which adequate visibility, gas composition and temperature are ensured [3, 4]. The evacuation route is also affected by the conditions of fire development in the surroundings [5, 6]. Additional elements are the issues related to fire resistance of building structures and their components [7–9]. The design of fire protection systems in underground objects is a complex, multi-stage issue, which creates many problems for designers [10, 11]. That is because of the complex nature of the physical phenomena that accompany the formation and development of a fire, against the effects of which the fire protection system should provide protection. A useful tool for assessing the performance of fire ventilation systems at the design stage is conducting thermal-flow analyses using the computational fluid mechanics CFD to recreate the conditions occurring in a building during a fire [12–14].

Modelling is carried out at various scales from micro [15] to real objects [1, 13, 16]. A methodology based on an automated optimization technique that uses a genetic algorithm is developed to estimate the material properties needed for CFD-based fire growth modelling from bench-scale fire test data [17]. Of particular interest is the modelling of shelter-type objects [11, 18, 19]. In this case, it is difficult to talk about fire ventilation and escape route. Air conditioning systems are limited to ensuring the right temperature, humidity and air velocity in the spaces. In modern shelters, there is no ventilation, the air composition is prepared by removing harmful gases on the principle of adsorption, while oxygen is supplied from cylinders. Consequently, the appearance of a fire outside a shelter comes down to an analysis of the temperature distribution inside the structure of the object [20].

The subject to analysis was the shelter housing strain due to external fire on the ground surface [21]. The numerical projection was carried out for a separated area covering the longitudinal, dug shelter together with the surrounding land [22]. It was assumed that the fire covered an extensive area which allowed one to adopt a geometric model in the analysis in the form of a flat, heterogeneous shield with the width equal to the size of the shelter increased on both sides by ΔL. The shield structure covers the shelter filled with air, monolithic, reinforced concrete housing and an adjacent land limited in the part above the ceiling level with a specified thickness of the covering layer equal to Δh. During the shelter construction, main and structural reinforcement was neglected due to the assumed approach assuming that heat conduction is determined by the thermodynamic properties of concrete. At the edge of the top shield, we assumed the environment temperature. Bottom edge of the shield was situated below the foundation slab level. It was positioned at the depth ensuring low sensitivity of the numeric analysis to its location. The analysed shield model was presented in Fig. 1.

Numerical calculations were performed using an author's own program written in the Turbo Pascal. The numerical analysis was carried out in two stages. In the first stage, a quasi-stationary initial temperature distribution was sought in the ground

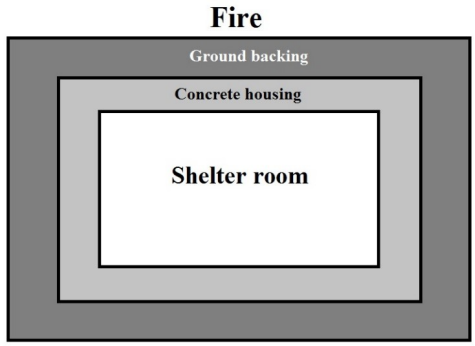

Fig. 1. Heterogeneous shield model

centre and shelter shield. It was assumed that this condition is determined by two factors: proper air temperature in the summer time as well as thermal effect of the protected resources and shelter crew, which after filling will be completely hermitic. It has been assumed that air temperature in the summer time is $t_0 = 22^\circ\text{C}$. The initial temperature in the ground centre, housing and shelter room was assumed to be $t_{\text{shelter}} = 12^\circ\text{C}$. At the same time, a function of temperature increase was assumed in the shelter room. Temperature increase is due to heat generated by shelter users. It is assumed that the shelter room temperature after one day reaches the stationary distribution in the form of a linear function at the room's height. This function spans across the ordinates at the floor and ceiling level, (t_{floor}, t_{ceiling}). The edge values of these temperatures were assumed, $t_{\text{ceiling}} = 28^\circ\text{C}$ and $t_{\text{floor}} = 0.8t_{\text{ceiling}}$. Further, stationary nature of this distribution is ensured by shelter's air conditioning system. After 4.5 days, quasi stationary temperatures were reached in the analysed shield – the housing and the surrounding land.

In the second stage of analysis, the fire effect was considered according to the time profile of temperature variation as per [23–25]. This profile covers the change of higher fire temperatures over a certain period $\tau_{iP} \leq \tau \leq \tau_{kP}$. We will define this period as the pre-heating, after the elapse of which the period of external air cooling will commence. In the cooling period ($\tau > \tau_{kP}$), we will assume that the external temperature will be described according to the adequate equation of Gauss curve falling branch.

$$t_P(\tau) = t_{\max}\left[1 - 0.325e^{-0.167(\tau-\tau_{iP})} - 0.675e^{-0.675(\tau-\tau_{iP})}\right] + t_0, \tag{1a}$$

$$t_P(\tau) = t(\tau_{kP})e^{b(\tau-\tau_{kP})\mp c(\tau-\tau_{kP})^2} + t_{\text{asympt}}\,. \tag{1b}$$

In Eq. (1a), the initial air temperature prior to the fire equals t_0, and in Eq. (1b) t_{asympt} becomes the temperature of the post-fire extinction. $t_{\text{asympt}} = 30^\circ\text{C}$ was assumed for numeric analysis.

2. Theoretical formulations and solution methodology

A non-stationary heat condition process was considered based on Fourier equation with the constant, average temperature adjustment in individual shield areas.

$$\frac{\partial^2 t}{\partial x^2} + \frac{\partial^2 t}{\partial z^2} = \frac{1}{a}\frac{\partial t}{\partial \tau}, \tag{2}$$

where: $a = \dfrac{\lambda}{\rho c_a}$ – average temperature balancing factor dependent upon λ heat conduction factor, proper heat c_a and volume density ρ of the ground or concrete.

Equation (2) is solved using a differentiation method combined with an open integration scheme and assumed temperature distributions – in the first stage of initial conditions determination in the shield according to item 2 and in the second stage of fire interaction ((1a), (1b)) on the surface level subject to temperature continuity in the shield at $\tau = \tau_{iP}$.

The spatial division of Δx and Δz and the time step of Δt was introduced, which ensure stability of numeric procedure and consistency of differentiation solution. The evolution formulas of the grid temperature were derived using the energy balance method of A.P. Waniczew [21, 26], for convenient analysis of areas with thermodynamically heterogeneous properties. Presented below are evolution formulas in the characteristic grid points.

A system of nods included in the elementary energy balance for nod (I, J=2) is presented in Fig. 2. We assumed that temperature assumption factor from the fire air area into the ground is $\alpha_{\text{air-ground}} = 2.4\ \dfrac{\text{W}}{\text{m}^2\text{K}}$.

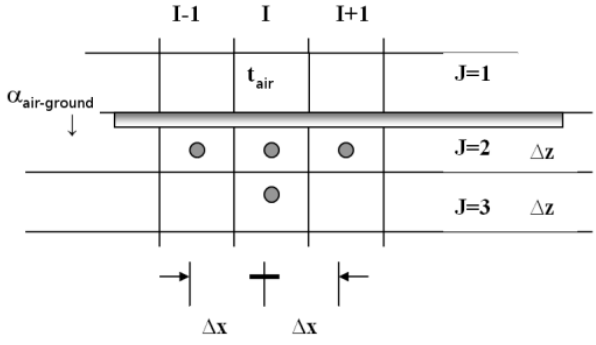

Fig. 2. The system of nods participating in the elementary energy balance for nod (I, J = 2)

The balance of elementary energies is expressed by the following equation (3) which takes into account $t^n(\text{I}-1, 2) = t^n(\text{I}, 2) = t^n(\text{I}+1, 2)$, as a consequence of the

assumption of the extensive fire area.

$$\Delta x \frac{t^n(\mathrm{I},3) - t^n(\mathrm{I},2)}{\dfrac{\Delta z}{\lambda_{\text{ground}}}} \Delta\tau - \Delta x \frac{t^n(\mathrm{I},2) - t(\mathrm{I},1)}{\dfrac{1}{\alpha_{\text{air-ground}}} + \dfrac{\Delta z}{2\lambda_{\text{ground}}}} \Delta\tau = \rho_{\text{ground}} c_a \Delta x \Delta z \left[t^{n+1}(\mathrm{I},2) - t^n(\mathrm{I},2) \right]. \tag{3}$$

Heat penetration factors from the fire into the ground and back were varied. The thermal energy balance equation after the insertion in $t^n(\mathrm{I},1) = t^n_{\text{air}}$, is as follows

$$t^{n+1}(\mathrm{I},2) = \left[1 - \frac{1}{M_{z,\text{ground}}} \left(1 + \frac{1}{N_{z,\text{air-ground}}} \right) \right] t^n(\mathrm{I},2) + \frac{1}{M_{z,\text{ground}}} \left[\frac{t^n_{\text{air}}}{N_{z,\text{air-ground}}} + t^n(\mathrm{I},3) \right], \tag{4}$$

where:

$$M_{z,\text{ground}} = \frac{\Delta z^2}{a_{\text{ground}} \Delta\tau}, \tag{5a}$$

$$N_{z,\text{air-ground}} = \frac{1}{2} + \frac{1}{\Delta \mathrm{Bi}_{z,\text{ground}}}. \tag{5b}$$

In Eq. (5b) $N_{z,\text{air-ground}}$ is defined using the Biot number,

$$\Delta \mathrm{Bi}_{z,\text{ground}} = \frac{\alpha_{\text{air-ground}} \Delta z}{\lambda_{\text{ground}}}. \tag{6}$$

The case where the nod and its surrounding areas remain in a homogeneous area, for example in the ground.

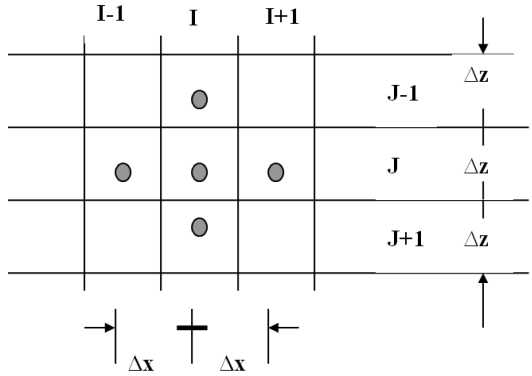

Fig. 3. A system of nods participating in the elementary energy balance

Based on the energy balance equation, we will be able to calculate the following:

$$t^{n+1}(\mathrm{I},\mathrm{J}) = \left[1 - 2\left(\frac{1}{M_{z,\mathrm{ground}}} + \frac{1}{M_{x,\mathrm{ground}}}\right)\right] t^{n}(\mathrm{I},\mathrm{J}) + \frac{1}{M_{x,\mathrm{ground}}}\left[t^{n}(\mathrm{I}\text{-}1,\mathrm{J}) + t^{n}(\mathrm{I}\text{+}1,\mathrm{J})\right] + \frac{1}{M_{z,\mathrm{ground}}}\left[t^{n}(\mathrm{I},\mathrm{J}\text{-}1) + t^{n}(\mathrm{I},\mathrm{J}\text{+}1)\right], \tag{7}$$

where:

$$M_{x,\mathrm{ground}} = \frac{\Delta x^2}{a_{\mathrm{ground}}\Delta\tau},$$

$$M_{z,\mathrm{ground}} = \frac{\Delta z^2}{a_{\mathrm{ground}}\Delta\tau},$$

$$a_{\mathrm{ground}} = \frac{\lambda_{\mathrm{ground}}}{\rho_{\mathrm{ground}} c_a}.$$

Nod within the external land cover directly adjacent to concrete (I, J=JOB)

Separate analysis is required with respect to nod situated directly in the neighbourhood of the ground and concrete housing borders area. The formula presented below allows us to calculate the evolution of temperature in the nod situated in the ground cover in the J=JOB layer adjacent to the concrete housing. We will use the geometric model given below.

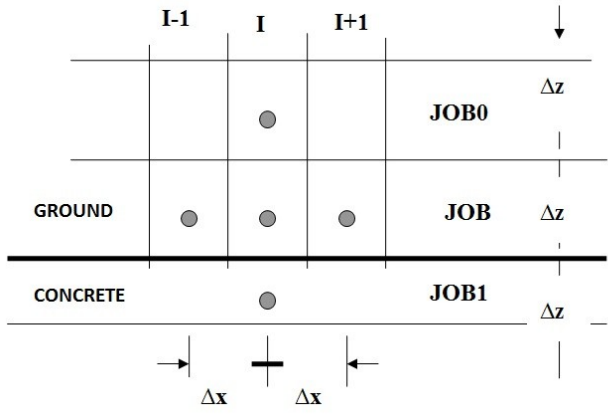

Fig. 4. The system of nods participating in the elementary energy balance

Based on the energy balance, we obtain a formula representing the temperature evolution in the nod (I, JOB)

$$t^{n+1}(\mathrm{I},\mathrm{JOB}) = \left[1 - \left(\frac{2}{1+\dfrac{\lambda_{\mathrm{ground}}}{\lambda_C}} + 1\right)\frac{1}{M_{z,\mathrm{ground}}} - \frac{2}{M_{x,\mathrm{ground}}}\right] t^n(\mathrm{I},\mathrm{JOB}) + \frac{1}{M_{z,\mathrm{ground}}}\left[\left(\frac{2}{1+\dfrac{\lambda_{\mathrm{ground}}}{\lambda_C}}\right) t^n(\mathrm{I},\mathrm{JOB1}) + t^n(\mathrm{I},\mathrm{JOB0})\right] + \frac{t^n(\mathrm{I1},\mathrm{JOB}) + t^n(\mathrm{I0},\mathrm{JOB})}{M_{x,\mathrm{ground}}}, \tag{8}$$

where λ_C is concrete thermal conductivity. In the next step we determine the temperature evolution formulas in the remaining areas of the shield.

3. Results and discussions

The shield of the thickness equal to $\Delta h = 0.4$ m and axial dimensions of the elements constituting the housing $L = 6.00$ m and $H = 2.80$ m was considered. In the numerical analysis, it was established that the thermal interactions included, in principle, the near surface strip of the total thickness equal to the thickness of the cover and the housing ceiling, i.e., $\Delta h + 0.40$ m. This observation was used to determine the thermal effect on the housing. It was therefore justified to burden with the temperature changes only the housing ceiling – the main upper frame rafter.

Two cases we considered. In the first one, the fire with the following parameters was considered: $t_{\max} = 650^{\circ}$C, $\tau_{\max} = \tau_{kP} - \tau_{iP} = 2$ h. It was assumed that the thickness of the ground cover was $\Delta h_1 = 0.40$ m. The numeric results including the analysis stage, whose aim was to determine the initial conditions of the shield at the break of the fire and the stage of pre-heating and cooling of fire temperatures are given in Fig. 5. Individual temperature variation curves represent selected layers: sub-ceiling and five internal ceiling layers. The black line represents the extreme, external ceiling layer.

The system of curves in the initial stage is reflected by the temperature distribution in the shield aiming at stabilisation. We assumed that these temperatures constitute long-term effect on the shelter housing and the results of such influence are subject to relaxation. For this reason, we do not consider them when predicting the initial shelter strain. We look for strain increase due to the occurrence of fire [23, 24].

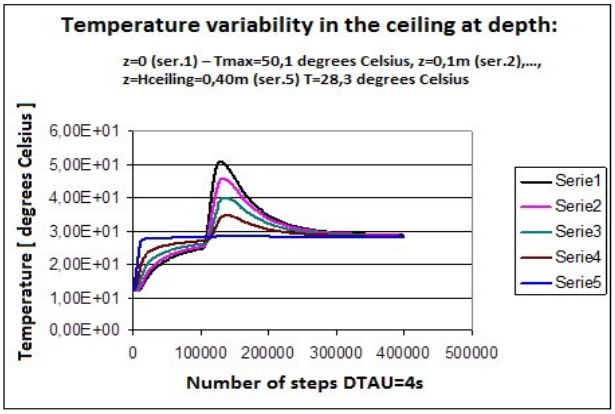

Fig. 5. Temperature variability in the sub-ceiling and five internal layers in the stage of determining the initial conditions of the analysis and the stage of influence of fire (650°C, 2 h)

Based on the analysis, the temperature increases due to fire were evaluated: on the ceiling surface (internal temperature) $\Delta t_{\text{int}} = 25.5^{\circ}\text{C}$ and on the external surface (outside temperature) $\Delta t_{\text{ext}} = 3.7^{\circ}\text{C}$. The shape of the bending moments and longitudinal forces due to load: altogether, the load of the cover, side thrust onto the housing walls, own weight of the housing and temperature effect (Δt_{int}, Δt_{ext}) on the frame rafter is given in Fig. 6.

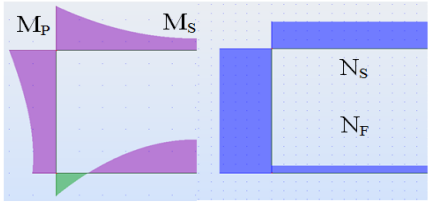

Fig. 6. The shape of the internal force diagram within the housing structure

Characteristic ordinate values are as follows:

$$\begin{aligned} &\text{bending moments } M_P = -111.11 \text{ kNm/m}, \quad M_S = -30.11 \text{ kNm/m}, \\ &\text{longitudinal forces } N_S = -38.18 \text{ kN/m}, \quad N_F = -10.51 \text{ kN/m}. \end{aligned} \tag{9}$$

Values due to temperature are equal:

$$M_P = M_S = -74.41 \text{ kNm/m}, \quad N_S = -N_F = -31.92 \text{ kN/m}. \tag{10}$$

From the comparison of (9) and (10) we can draw a conclusion that the share of thermal influence in the strain of the critical cross-sections of the raft is

considerable. This comment pertains in particular to critical cross-sections of the upper node of the frame. The occurrence of the compressive force in the main rafter is used due to tightness of the housing. In the other case, fire with the following parameters was considered: $t_{\max} = 1600^{\circ}\mathrm{C}$ and $\tau_{\max} = 1.5$ h. It was necessary to assume the cover of increased thickness of $\Delta h_2 = 0.60$ m. Analogous temperature variability in the housing ceiling layers is presented in Fig. 7.

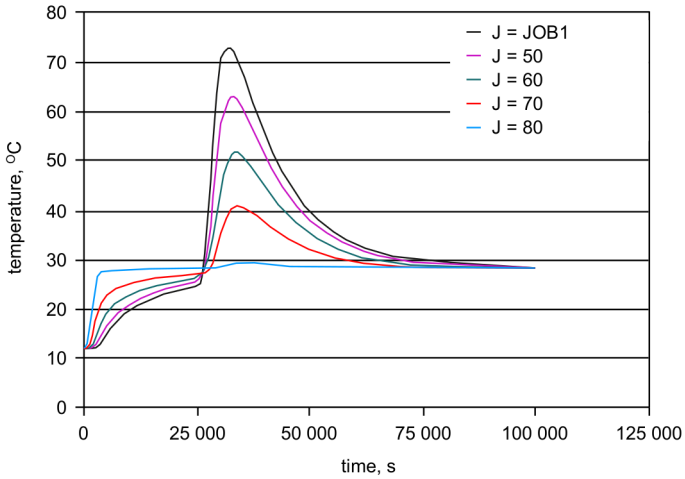

Fig. 7. Temperature variability in sub-ceiling and five internal ceiling layers in the stages of determining initial analysis conditions and fire influence stage (1600°C, 1.5 h)

As in the preceding case, we look for temperature increases in the housing frame rafter due to fire. This can be estimated in the following way: $\Delta t_{\mathrm{int}} = 47.7^{\circ}\mathrm{C}$ and $\Delta t_{\mathrm{ext}} = 4.6^{\circ}\mathrm{C}$. The characteristic values of the ordinates of the internal force diagrams are as follows:

$$\text{bending moments } M_P = -190.71 \text{ kNm/m}, \quad M_S = -91.71 \text{ kNm/m},$$
$$\text{longitudinal forces } N_S = -70.62 \text{ kN/m}, \quad N_F = 17.06 \text{ kN/m}.$$

The values due to temperature are equal:

$$M_P = M_S = -145.47 \text{ kNm/m}, \quad N_S = -N_F = -61.93 \text{ kN/m}.$$

4. Conclusions

The results of the numerical analyses indicate that the thickness of the soil layer should be determined according to the parameters of the fire when analysing the second case, a fire with parameters: $t_{\max} = 1600^{\circ}\mathrm{C}$ and it is necessary to adopt a soil layer with an increased thickness $\Delta h_2 = 0.60$ m. The most temperature-exposed ceiling of the shelter suffers a considerable compression as the above results show.

Bending upwards relieves the load on the middle section due to bending, at the same time adversely burdens the node of the monolithic confirmation of the ceiling in the wall.

Manuscript received by Editorial Board, March 07, 2021;
final version, June 05, 2021.

References

[1] A. Dorsz, A. Rusowicz, and A. Prawdzik. Comparative analysis of assumptions for numerical simulation of the effects of fire – safety of evacuation from the building structure. *Inżynieria Bezpieczeństwa Obiektów Antropogenicznych*, 4(2020):212–226, 2020 doi: 10.37105/iboa.89.

[2] A. Asgary, A.S. Naini, and J. Levy. Intelligent security systems engineering for modeling fire critical incidents: towards sustainable security. *Journal of Systems Science and Systems Engineering*, 18(4):477–488, 2009. doi: 10.1007/s11518-009-5121-2.

[3] J.L. Coen. Some new basics of fire behavior. *Fire Management Today*, 71(1):38–43, 2011.

[4] T. Putnam and B.W. Butler. Evaluating fire shelter performance in experimental crown fires. *Canadian Journal of Forwst Research*, 34(8):1600–1615, 2004. doi: 10.1139/X04-091.

[5] E. Ozbay, Ö. Çavus, and B.Y. Kara. Shelter site location under multi-hazard scenarios. *Computers and Operations Research*, 106:102–118, 2019. doi: 10.1016/j.cor.2019.02.008.

[6] R. Linn, K. Anderson, J. Winterkamp, A. Brooks, M. Wotton, J-L. Dupuy, F. Pimont, and C. Edminster. Incorporating field wind data into FIRETEC simulations of the International Crown Fire Modeling Experiment (ICFME): preliminary lessons learned. *Canadian Journal of Forest Research*, 42(5):879–898, 2012. doi: 10.1139/X2012-038.

[7] Ch. Zhang, J.G. Silva, C. Weinschenk, D. Kamikawa, and Y. Hasemi. Simulation methodology for coupled fire-structure analysis: modeling localized fire tests on a steel column. *Fire Technology*, 52:239–262, 2016. doi: 10.1007/s10694-015-0495-9.

[8] T. Molkens and B. Rossi. On the simulation of real fire for post fire resistance evaluation of steel structures. *Fire Technology*, 57:839–871, 2021. doi: 10.1007/s10694-020-01025-6.

[9] N. Johansson, J. Anderson, R. McNamee, and Ch. Pelo. A Round Robin of fire modelling for performance-based design. *Fire and Materials*, 2020:1–14, doi: 10.1002/fam.2891.

[10] J. Lu, T. Wang, L. Wang, W. Chen, and Y. Chen. Optimization of duct structure and analysis of its impact on temperature inside the shelter. *Journal of Physics: Conference Series*, 1300:012011, 2019. doi: 10.1088/1742-6596/1300/1/012011.

[11] A.Baryłka. The impact of fire on changing the strength of the underground shelter structure. *Rynek Energii*, 146(1):71–75, 2020.

[12] T.J. Cova, P.E. Dennison, and F.A. Drews. Modeling evacuate versus shelter-in-place decisions in wildfires. *Sustainability*, 3(10):1662–1687, 2011. doi: 10.3390/su3101662.

[13] M.D. Lulea, V. Iordache, and I. Năstase. Fire modeling in a nonventilated corridor. *E3S Web of Conferences*, 32:01011, 2018. doi: 10.1051/e3sconf/20183201011.

[14] C. Salter. Fire modelling within cloud based resources. *Fire Technology*, 51:491–497, 2015. doi: 10.1007/s10694-014-0433-2.

[15] M. Krajčír and J. Müllerová. 3D small-scale fire modeling experiments. *Procedia Engineering* 192:474–479, 2017. doi: 10.1016/j.proeng.2017.06.082.

[16] Y. Varaksin. Concentrated air and fire vortices: Physical modeling (a review). *High Temperature*, 54(3):409–427, 2016. doi: 10.1134/S0018151X16030226.

[17] Ch. Lautenberger, G. Rein, and C. Fernandez-Pello. The application of a genetic algorithm to estimate material properties for fire modeling from bench-scale fire test data. *Fire Safety Journal*, 41(3):204–214, 2006. doi: 10.1016/j.firesaf.2005.12.004.

[18] A. Dorsz and A.Rusowicz. Numerical modelling of the influence of thermal effects on the exhaust fans in the fire ventilation systems. *Rynek Energii*, 154(3):85–90, 2021. (in Polish).
[19] J.A. Prusiel. Theoretical and experimental analysis of thermal fields distribution in granular media stored in silo model. *Acta Agrophysica*, 19(2):391–402, 2012. (in Polish).
[20] PN-EN: 1991-1-2:2006 – Actions on structures exposed to fire.
[21] Z. Garncarek and J. Idzik. Degree of heterogeneity of thermal field a method of evaluation. *International Journal of Heat and Mass Transfer*, 35(11):2769–2775, 1992. doi: 10.1016/0017-9310(92)90297-6.
[22] A. Baryłka and D. Tomaszewicz. Influence of measuring deviations of the components of layered walls on their durability. *Inżynieria Bezpieczeństwa Obiektów Antropogenicznych*, 3(2020):155–162, 2020. doi: 10.37105/iboa.75.
[23] M. Abramowicz. Design of building structures subject to fire exposure according to Eurocodes. *Kalendarz budowlany 2008 r.* chapter 18. Warszawskie Centrum Postępu Techniczno-Organizacyjnego Budownictwa WACETOB. (in Polish)
[24] A.Baryłka. The issue of the fitness of buildings for use in the issues of safety engineering of these objects. *Inżynieria Bezpieczeństwa Obiektów Antropogenicznych*, 4, 2019, (in Polish). doi: 10.37105/iboa.31.
[25] A. Baryłka and D. Tomaszewicz. Influence of surface shape of glued anchors on their load capacity. *Modern Engineering*, 2:78–82, 2020.
[26] E. Kostowski. *Heat Flow*. WPŚL, Gliwice, 2000. (in Polish).